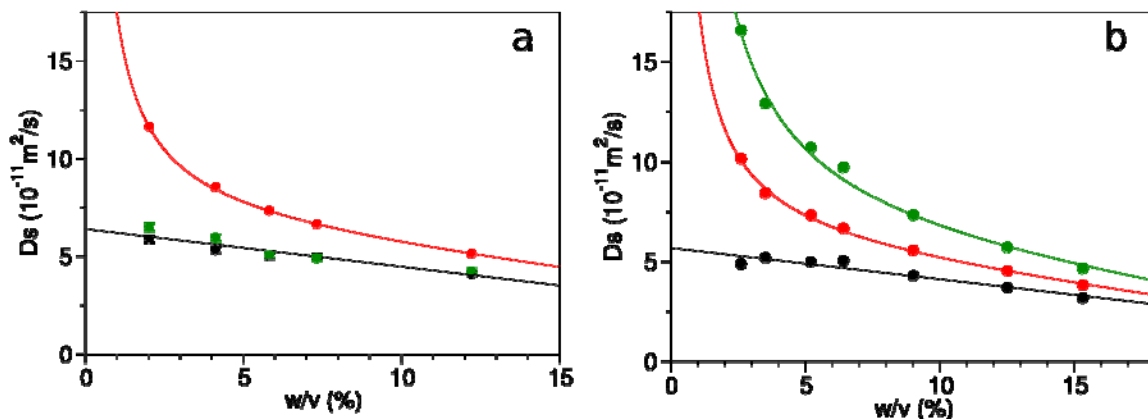


## Supplementary Information

**Supplemental Materials and Methods.**  $^1\text{H}$  and  $^{31}\text{P}$  diffusion measurements were conducted using bipolar gradient pulse pairs in a longitudinal eddy current delay experiment (BPP-LED) (Wu et al. 1995; Chou et al. 2004) on a 500-MHz NMR Bruker Avance III spectrometer using a QXI  $^1\text{H}/^{31}\text{P}/^{13}\text{C}/^{15}\text{N}/^2\text{H}$  probe with three-axis gradients. A combination of x- and z-axis gradients was applied during the encoding and decoding periods, and reported diffusion constants were calibrated against those of a hen egg-white (HEW) lysozyme sample of the same composition as used by Chou et al. (2004). Diffusion experiments were conducted at 298.0 K.



**Fig. S1** Translational diffusion rates,  $D_s$ , of the components of small charged bicelles as a function of total weight fraction of lipid plus detergent. Translational diffusion measurements were conducted at 298 K, using a  $^{31}\text{P}$  BPP-LED experiment at 500 MHz. Shown are the diffusion rates obtained from fitting the intensity decay of the resolved phosphocholine  $^{31}\text{P}$  peaks for DMPC (black), DOHPC (red) and DMPS (green, a) or the overlapped resonances of DMPS and DHPS (green, b). (a) The bicelle sample had an initial concentration of 60 mM DMPC, 162 mM DOHPC and 19 mM DMPS ( $q = 0.49$ ) in 25 mM Tris pH 7.4 and 7%  $\text{D}_2\text{O}$ . The lipid concentration was changed by diluting the bicelle samples with 25 mM Tris pH 7.4 and 6%  $\text{D}_2\text{O}$ . The extrapolated bicelle translational diffusion rate at infinite dilution,  $D_0$ , is  $6.4 \cdot 10^{-11} \text{ m}^2/\text{s}$ , as measured by the diffusion rates of DMPC and DMPS. The DOHPC is in fast equilibrium between bicelle-bound and free-monomer states, the latter of which has a diffusion rate of  $43.8 \cdot 10^{-11} \text{ m}^2/\text{s}$  (Chou et al. 2004). The difference between the DOHPC translational diffusion rate and that of the 100%-bicelle-bound DMPC is used to determine the fraction of free DOHPC (Chou et al. 2004), yielding a free-monomer concentration of *ca* 7 mM. This value is comparable to the free DHPC concentration of 5 mM measured for DMPC/DHPC bicelles (Chou et al. 2004), and considerably lower than its critical micelle concentration (cmc) of *ca* 14 mM. (b) The bicelle sample had an initial concentration of 61 mM DMPC, 164 mM DOHPC, 19 mM DMPS and 64 mM DHPS in 25 mM Tris pH 7.3 and 6%  $\text{D}_2\text{O}$  ( $q=0.35$ ), and was stepwise decreased by dilution with buffer. The extrapolated bicelle translational diffusion rate at infinite dilution,  $D_0$ , is  $5.7 \cdot 10^{-11} \text{ m}^2/\text{s}$ . The DOHPC free-monomer concentration is fitted to be 8 mM. The free monomer concentration of DHPS cannot be accurately established due to its overlap with the DMPS resonance, and the intensity decay during the gradient diffusion experiment being insufficiently bi-exponential to resolve separate rate constants at the attainable signal-to-noise ratio. However, the steeper increase in the apparent DHPS/DMPS upon dilution compared to DOHPC indicates a larger free concentration for DHPS than for DOHPC (in agreement with its higher cmc of *ca* 24 mM in Tris buffer (N.A. Bax, unpublished results), thereby somewhat increasing the effective  $q$ -ratio and the size of the bicelle upon diluting the sample with buffer.

**Table S1** Experimental  $^1\text{H}$ - $^{15}\text{N}$  RDCs for HAfp23 in different bicelle formulations aligned by stretched acrylamide gel and K-d(GpG)<sup>a,b,c</sup>

	A	B	C	D	E	F	G	H	I
Phe3	25.2	21.3	13.4	18.5	17.0	-16.6	-11.5	-10.1	-23.3
Gly4	20.8	20.6	14.4	15.5	16.3	-8.6	-6.1	-7.1	-16.1
Ala5	1.4	5.7	7.5	1.3	8.4	9.1	4.5	1.4	5.5
Ile6	8.0	6.8	5.6	4.1	5.8	-0.9	-1.7	0.1	-4.1
Ala7	21.1	18.9	13.0	14.7	15.8	-10.3	-7.9	-8.0	-18.6
Gly8	7.6	10.5	11.2	6.2	13.5	4.7	2.2	-0.9	-3.5
Ile10	10.4	9.0	7.8	6.2	10.7	0.4	0.7	-1.2	-3.5
Glu11	15.0	15.1	12.6	10.4	13.4	-3.5	-3.0	-4.8	-10.5
Gly12	-0.8	3.5	7.5	-0.1	5.3	12.7	5.8	2.8	9.9
Gly13	-23.3	-25.9	-15.6	-21.7	-18.5	17.9	17.8	18.0	24.4
Trp14	21.2	17.3	9.6	14.2	11.1	-14.2	-9.1	-7.4	-19.8
Thr15	17.0	16.6	13.1	12.1	12.5	-4.3	-3.6	-4.2	-11.2
Gly16	35.9	31.5	16.7	27.9	18.1	-29.0	-23.0	-20.0	-40.6
Met17	20.6	15.4	8.0	13.3	9.8	-14.8	-8.7	-6.6	-19.8
Ile18	11.0	10.1	8.2	6.0	9.4	-0.2	-0.5	-1.1	-5.7
Asp19	21.2	20.2	14.2	15.4	14.3	-10.8	-8.3	-5.4	-18.8
Gly20	31.9	26.1	13.0	23.0	15.5	-27.5	-19.6	-16.9	-34.9
Trp21	5.4	0.2	1.1	0.8	0.6	-0.5	3.1	3.4	-1.5
Tyr22	7.5	5.2	6.0	3.3	6.6	1.7	1.9	1.1	-3.0
Gly23	35.6	31.0	14.8	27.3	19.9	-30.1	-23.1	-19.5	-40.0
D <sub>a</sub>	18.8	-17.1	-10.1	15.4	-11.4	-17.8	-15.4	-13.1	-22.3
Rh	0.41	0.66	0.42	0.55	0.46	0.13	0.41	0.53	0.28

<sup>a</sup> The samples had the following compositions:

A. Neutral bicelles in SAG: 0.6 mM  $^2\text{H}$ ,  $^{13}\text{C}$ ,  $^{15}\text{N}$ -labeled HAfp23, 25 mM  $^2\text{H}$ -labeled Tris pH 7.3, 27 mM DMPC, 100 mM DOHPC, 16 mM DPC, 7% D<sub>2</sub>O in SAG (see Materials and Methods for details on the acrylamide gel formulation for this and other SAG samples).

B. Bicelles + DMPS in SAG: 0.7 mM  $^2\text{H}$ ,  $^{13}\text{C}$ ,  $^{15}\text{N}$ -labeled HAfp23, 25 mM  $^2\text{H}$ -labeled Tris pH 7.3, 46 mM DMPC, 160 mM DOHPC, 8.1 mM DMPS, 10 mM DPC, 7% D<sub>2</sub>O in SAG.

C. Bicelles + DMPS + DHPS in SAG: 0.7 mM  $^2\text{H}$ ,  $^{13}\text{C}$ ,  $^{15}\text{N}$ -labeled HAfp23, 25 mM  $^2\text{H}$ -labeled Tris pH 7.3, 46 mM DMPC, 160 mM DOHPC, 8.1 mM DMPS, 46 mM DHPS, 10 mM DPC, 7% D<sub>2</sub>O in SAG.

D. Bicelles + Et-DMPC in SAG: 0.6 mM  $^2\text{H}$ ,  $^{13}\text{C}$ ,  $^{15}\text{N}$ -labeled HAfp23, 25 mM  $^2\text{H}$ -labeled Tris pH 7.4, 42 mM DMPC, 150 mM DOHPC, 10 mM Et-DMPC, 10 mM DPC, 7% D<sub>2</sub>O in SAG.

E. Medium-sized bicelles in SAG: 0.7 mM  $^2\text{H}$ ,  $^{13}\text{C}$ ,  $^{15}\text{N}$ -labeled HAfp23, 25 mM  $^2\text{H}$ -labeled Tris pH 7.0, 73 mM DMPC, 144 mM DOHPC, 16 mM DPC, 7% D<sub>2</sub>O in SAG.

F. Neutral bicelles in d(GpG): 0.3 mM  $^{13}\text{C}$ ,  $^{15}\text{N}$ -labeled HAfp23, 25 mM  $^2\text{H}$ -labeled Tris pH 7.3, 22 mM DMPC, 65 mM DOHPC, 10 mM DPC, 15 mg/ml d(GpG), 60 mM KCl, 7% D<sub>2</sub>O.

G. Bicelles + DMPS in d(GpG): 0.3 mM  $^{13}\text{C}$ ,  $^{15}\text{N}$ -labeled HAfp23, 25 mM  $^2\text{H}$ -labeled Tris pH 7.4, 22 mM DMPC, 85 mM DOHPC, 6 mM DMPS, 10 mM DPC, 15 mg/ml d(GpG), 60 mM KCl, 7% D<sub>2</sub>O.

H. Bicelles + DMPS + DHPS in d(GpG): 0.3 mM  $^{13}\text{C}$ ,  $^{15}\text{N}$ -labeled HAfp23, 25 mM  $^2\text{H}$ -labeled Tris pH 7.4, 22 mM DMPC, 85 mM DOHPC, 6 mM DMPS, 27 mM DHPS, 10 mM DPC, 15 mg/ml d(GpG), 60 mM KCl, 7% D<sub>2</sub>O.

I. Bicelles + Et-DMPC in d(GpG): 0.3 mM  $^{13}\text{C}$ ,  $^{15}\text{N}$ -labeled HAfp23, 25 mM  $^2\text{H}$ -labeled Tris pH 7.3, 25 mM DMPC, 82 mM DOHPC, 6 mM Et-DMPC, 10 mM DPC, 15 mg/ml d(GpG), 60 mM KCl, 7% D<sub>2</sub>O.

<sup>b</sup> RDCs and D<sub>a</sub>s are in units of Hz, and the rhombicities (Rh) are unitless. The D<sub>a</sub>/Rh are calculated from a SVD of the RDCs to the HAfp23 structure with PDB accession code 2KXA (Lorieau et al. 2010). The experimental error scales approximately with D<sub>a</sub>, and for a D<sub>a</sub> = 10 Hz, the experimental uncertainty is estimated to be ~0.5 Hz.

<sup>c</sup> The RDC for Phe9 was not included due to spectral overlap with Lys residues from the polyionic host fragment of the peptide.

**Table S2** Saupe alignment tensor components obtained after tensors F-I from Table 1 have been orthogonalized, using the unitary matrix of Table S5.<sup>a,b,c</sup>

Component/Tensor	Tensor 1	Tensor 2	Tensor 3	Tensor 4
$S_{zz}$	-13.07	-4.41	-1.02	0.17
$(1/\sqrt{3})(S_{xx} - S_{yy})$	22.17	0.57	-1.69	0.84
$(2/\sqrt{3})S_{xy}$	-3.51	4.29	-1.18	-0.82
$(2/\sqrt{3})S_{xz}$	29.49	-2.64	0.19	-0.96
$(2/\sqrt{3})S_{yz}$	-12.61	-1.79	-1.15	-0.70

<sup>a</sup> See Table S1 for a legend of the sample compositions.

<sup>b</sup> Tensor components are in units of Hz and have been generated by SVD of the tensors from Table 1, after scaling these to a  $D_a$  of 10 Hz.

<sup>c</sup> The SVD of matrix M, composed of the tensors F-I in Table S2, produces three matrices, U,  $\Sigma$ ,  $V^*$ . The diagonal components of  $\Sigma$  are the singular values, which when multiplied by the columns of the unitary matrix U (Table S5) produces the orthogonalized tensors. The matrix  $V^*$  is presented in Table S8.

**Table S3** Saupe alignment tensor components obtained after tensors A-E from Table S2 have been orthogonalized, using the unitary matrix of Table S6.<sup>a,b</sup>

Component/Tensor	Tensor 1	Tensor 2	Tensor 3	Tensor 4	Tensor 5
$S_{zz}$	-20.86	-3.88	1.56	-0.32	-0.03
$(1/\sqrt{3})(S_{xx} - S_{yy})$	13.03	-7.01	-1.14	0.32	0.00
$(2/\sqrt{3})S_{xy}$	-6.00	1.67	-1.84	-0.43	-0.04
$(2/\sqrt{3})S_{xz}$	32.91	-0.68	0.51	-0.86	0.00
$(2/\sqrt{3})S_{yz}$	-24.03	-1.77	-0.82	-0.62	0.03

<sup>a</sup> See Table S1 for a legend of the sample compositions.

<sup>b</sup> Tensor components are in units of Hz and have been generated by SVD of the tensors from Table 1, after scaling these to a  $D_a$  of 10 Hz.

**Table S4** Experimental  $^1\text{H}$ - $^{15}\text{N}$  RDCs (in units of Hz) transformed to the frames of the orthogonalized Saupe matrices from Table 3, using the transformation matrix of Table S10.

Residue/Tensor	I	II	III	IV	V
Phe3	-33.58	-5.61	-4.78	-0.32	1.04
Gly4	-27.82	-10.19	-4.22	-0.85	0.53
Ala5	-2.87	-12.44	-0.26	-0.31	0.50
Ile6	-8.32	-4.99	-2.34	-1.39	0.24
Ala7	-28.01	-7.83	-4.10	-0.44	0.49
Gly8	-11.89	-14.04	-2.38	0.26	-0.06
Ile10	-11.32	-9.21	-3.01	-0.56	1.48
Glu11	-20.10	-10.49	-3.10	-0.50	0.17
Gly12	1.10	-12.85	0.79	-1.49	0.12
Gly13	39.97	5.20	-0.66	-1.18	-0.66
Trp14	-26.09	-2.39	-4.56	-1.21	0.37
Thr15	-21.28	-10.11	-3.69	-1.75	-0.01
Gly16	-50.92	0.32	-3.90	-0.95	-0.73
Met17	-24.30	-0.78	-4.99	-1.15	0.47
Ile18	-12.02	-8.32	-3.11	-1.28	0.42
Asp19	-27.93	-8.03	-5.09	-1.59	-0.48
Gly20	-43.40	1.80	-4.34	-0.33	0.37
Trp21	-0.45	-1.43	-4.01	-1.54	0.41
Tyr22	-6.43	-7.08	-3.24	-1.04	0.24
Gly23	-50.53	0.82	-4.37	-0.08	0.53

**Table S5** The SVD unitary matrix (U) used to generate the orthogonalized tensors in Table S2.<sup>a,b</sup>

-0.3167	-0.6344	-0.3942	0.1008	-0.5759
0.5372	0.0827	-0.6559	0.5019	0.1503
-0.0850	0.6169	-0.4583	-0.4883	-0.4046
0.7146	-0.3797	0.0730	-0.5696	-0.1244
-0.3055	-0.2568	-0.4462	-0.4184	0.6830

<sup>a</sup>The orthogonalized tensors are generated by multiplying the unitary matrix by the singular values 41.27, 6.95, 2.58, 1.68, 0.

**Table S6** The SVD unitary matrix (U) used to generate the orthogonalized tensors in Table S3.<sup>a</sup>

-0.4348	-0.4621	0.5503	-0.2594	-0.4768
0.2717	-0.8342	-0.4029	0.2570	-0.0440
-0.1251	0.1986	-0.6474	-0.3470	-0.6368
0.6860	-0.0805	0.1789	-0.6995	0.0395
-0.5009	-0.2112	-0.2895	-0.5069	0.6031

<sup>a</sup>The orthogonalized tensors are generated by multiplying the unitary matrix by the singular values 47.97, 8.40, 2.84, 1.23, 0.06.

**Table S7** The SVD unitary matrix (U) used to generate the orthogonalized tensors in Table 1.<sup>a</sup>

-0.3901	-0.4465	0.5120	0.0971	-0.6139
0.3917	-0.7583	-0.3516	0.3782	0.0692
-0.1099	0.0419	-0.7065	-0.3482	-0.6049
0.7087	-0.0973	0.3353	-0.5822	-0.1920
-0.4243	-0.4630	-0.0523	-0.6223	0.4643

<sup>a</sup>The orthogonalized tensors are generated by multiplying the unitary matrix by the singular values 62.32, 13.93, 7.24, 3.35, 0.96.

**Table S8** The matrix (V\*) from the SVD listed in the footnote to Table S2.

0.4748	0.5072	0.5246	0.4920
-0.6240	0.3556	0.5806	-0.3834
-0.5255	-0.3914	0.1621	0.7378
-0.3301	0.6805	-0.6012	0.2580

**Table S9** Normalized scalar products of the molecular alignment tensors of HAfp23 aligned in small bicelles of different charge and shape to the alignment tensors in DPC used for the structural refinement of the structure with PDB accession code 2KXA<sup>a</sup>

	DPC-SAG	DPC-d(GpG)
A: neutral bicelles in SAG	0.832	-0.891
B: bicelle + DMPS in SAG	0.700	-0.782
C: bicelle + DMPS + DHPS in SAG	0.582	-0.618
D: bicelle + Et-DMPC in SAG	0.744	-0.834
E: medium bicelles in SAG	0.633	-0.665
F: bicelles in d(GpG)	-0.877	0.957
G: bicelles + DMPS in d(GpG)	-0.700	0.842
H: bicelles + DMPS + DHPS in d(GpG)	-0.652	0.788
I: bicelles + Et-DMPC in d(GpG)	-0.850	0.925

<sup>a</sup> See Table S1 for a summary of sample compositions.

**Table S10** Transformation matrix from experimental RDCs to orthogonal RDC sets, yielding Table S4.

	A	B	C	D	E	F	G	H	I
I	-0.34	-0.37	-0.32	-0.35	-0.33	0.30	0.33	0.35	0.32
II	0.06	-0.16	-0.56	0.01	-0.49	-0.48	-0.30	-0.15	-0.25
III	-0.40	0.08	-0.02	0.04	-0.12	0.37	-0.46	-0.59	0.34
IV	-0.60	-0.24	0.08	-0.15	0.39	-0.52	0.25	-0.27	-0.07
V	0.43	-0.19	-0.24	0.04	0.32	-0.27	-0.02	-0.10	0.73

**Table S11** Normalized scalar products of the alignments tensors corresponding to RDC datasets obtained from direct orthogonalization (OLC) of a matrix composed from experimental RDCs measured in media A-H.

	I	II	III	IV	V
I					
II	0.548				
III	0.625	0.226			
IV	0.426	0.265	0.614		
V	0.213	0.322	0.443	0.800	
D <sub>a</sub>	-27.43	7.55	4.00	-1.09	-0.68
Rh	0.58	0.55	0.63	0.65	0.63

**Code Listing 1.** Matlab script for calculating RDC sets corresponding to the orthogonalized Saupe matrices.

```

% Alignment tensors for SAG samples in 5-component representation (see Table 1)
GelSaupe = [
    [ 11.0    17.6    11.4    13.3    12.0 ];
    [ -15.9   -13.3    -1.6   -13.9   -2.2];
    [   9.1     4.1     2.0     3.6     2.2 ];
    [ -27.8   -26.2   -13.5   -23.6   -16.9];
    [ 19.0     19.1    11.8    14.8    12.8]];

% Absolute values of Da for SAG samples for normalization purposes
DaGel = [ 18.8 17.1 10.1 15.4 11.4 ];

% Alignment tensors for GpG samples in 5-component representation (see Table 1)
GpGSaupe = [
    [-5.3   -11.8   -12.7  -12.1];
    [19.2    19.5    14.6   21.5];
    [-6.1    -0.5     1.2   -9.9];
    [28.2    20.5    19.1   34.4];
    [-7.2   -10.9   -9.7  -14.6]];

% Absolute values of Da for GpG samples for normalization purposes
DaGpG = [ 17.8 15.4 13.1 22.3 ];

% Merging SAG and GpG data together
AllSaupe = [GelSaupeOld GpGSaupeOld]
DaAll = [DaGel DaGpG ]

% Normalizing the experimental tensors to 10 Hz Da
for i=1:9
    AllSaupe(:,i) = AllSaupe(:,i) ./ (DaAll(i)/10);
end

% Performing SVD on alignment tensors that have been normalized to 10 Hz Da.
[U,S,V] = svd(AllSaupe);
invV = inv(V');
% The first 5 columns of AllSaupe*invV (or U*S) are the orthogonalized tensors
of Table 3.
% The remaining columns are zeros.

% Read in RDCs
fin=fopen('All_RDCs_new.prn');
% Format of each line in the file is residue number followed by 9 RDC values.
% Notice that the order of RDC columns matches the order of tensors above.
data_all=fscanf(fin, '%f %f %f %f %f %f %f %f %f %f', [10, Inf]);
fclose(fin);
res_nums = data_all(1, :); % Residue numbers in the RDC dataset
RDCsAll = data_all(2:10, :);

% Normalizing RDCs to 10 Hz Da. Must be done because the alignment tensors
% have been normalized to 10 Hz Da.
for i=1:9
    RDCsAll(:,i) = RDCsAll(:,i) ./ (DaAll(i)/10);
end

% Open the output file and save the row containing the residue numbers
fout=fopen('Orthogonal_RDCs.txt', 'w');
fprintf(fout, '%d\t', res_nums);
fprintf(fout, '\n');

% Generate the 5 orthogonalized RDC sets one by one.

```



```
for i=1:5
    Qs = invV(:, i);
    % Here AllSaupe*Qs yields the i-th orthogonalized tensor of Table 3.

    % Calculate the orthogonalized RDC set based on the same Qs.
    orthogonalRDCs = RDCsAll*Qs;

    % Save the RDC set as a single line in the output file.
    fprintf(fout, '%.2f\t', orthogonalRDCs);    fprintf(fout, '\n');
end

fclose(fout);
```

## References

- Chou, JJ, Baber, JL and Bax, A (2004) Characterization of phospholipid mixed micelles by translational diffusion. *J. Biomol. NMR* 29: 299-308.
- Lorieau, JL, Louis, JM and Bax, A (2010) The complete influenza hemagglutinin fusion domain adopts a tight helical hairpin arrangement at the lipid:water interface. *Proc. Natl. Acad. Sci. U. S. A.* 107: 11341-11346.
- Wu, DH, Chen, AD and Johnson, CS (1995) An improved diffusion-ordered spectroscopy experiment incorporating bipolar-gradient pulses. *Journal of Magnetic Resonance Series A* 115: 260-264.